Title

Conductance and Configuration of Molecular Gold-Water-Gold Junctions under Electric Fields

Authors

Xiang, Limin
Zhang, Peng
Liu, Chaoren
et al.

Peer reviewed

Conductance and configuration of molecular gold-water-gold junctions under electric fields

Limin Xiang[1,8,†,*], **Peng Zhang**[2], **Chaoren Liu**[2], **Xin He**[4], **Haipeng B. Li**[5], **Yueqi Li**[1], **Zixiao Wang**[7], **Joshua Hihath**[5], **Seong H. Kim**[4,*], **David N. Beratan**[2,3,*], **Nongjian Tao**[1,6,*,‡]

[1]Biodesign Center for Biosensors and Bioelectronics, Biodesign Institute, Arizona State University, Tempe, Arizona 85287, USA

[2]Departments of Chemistry and Physics, Duke University, Durham, North Carolina 27708, USA.

[3]Department of Biochemistry, Duke University, Durham, North Carolina 27710, USA

[4]Department of Chemical Engineering and Materials Research Institute, Pennsylvania State University, University Park, Pennsylvania 16802, USA

[5]Department of Electrical and Computing Engineering, University of California, Davis, Davis, California 95616, USA

[6]School of Electrical, Computer and Energy Engineering, Arizona State University, Tempe, Arizona 85287, USA

[7]State Key Laboratory of Analytical Chemistry for Life Science, School of Chemistry and Chemical Engineering, Nanjing University, Nanjing 210093, China

[8]Lead contact

Summary

Water molecules can mediate charge transfer in biological and chemical reactions by forming electronic coupling pathways. Understanding the mechanism requires a molecular-level electrical characterization of water. Here, we describe the measurement of single water molecular conductance at room temperature, characterize the structure of water molecules using infrared spectroscopy, and perform theoretical studies to assist in the interpretation of the experimental data. The study reveals two distinct states of water, corresponding to a parallel and perpendicular

[*]Correspondence to: Limin.Xiang@asu.edu; njtao@asu.edu; david.beratan@duke.edu; shkim@engr.psu.edu.
[†]Current Address: Department of Chemistry, University of California, Berkeley, CA, 94720, USA

Declaration of Interests

The authors declare no competing interests

Supplemental Information: Supplemental Information is linked to the online version of the paper.

orientation of the molecules. Water molecules switch from parallel to perpendicular orientations on applying an electric field, producing switching from high to low conductance states, thus enabling the determination of single water molecular dipole moments. The work further shows that water-water interactions affect the atomic scale configuration and conductance of water molecules. These findings demonstrate the importance of the discrete nature of water molecules in electron transfer and set limits on water-mediated electron transfer rates.

Graphical Abstract
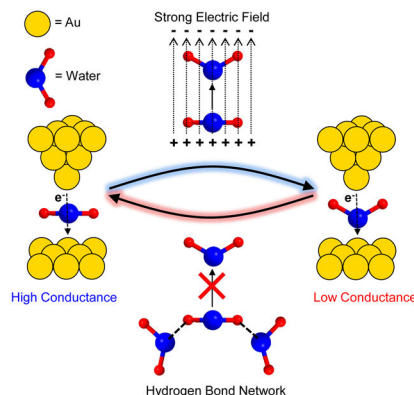
(3) An eTOC blurb no longer than 80 words describing the context and significance of the findings for the broader journal readership

Tao and colleagues found two conductance states for single water molecular junctions, originating with two water orientations that depend on water-water interactions. Electric fields can further switch the water molecular junction from the high to low conductance states. The study reveals the nature of water molecules as charge mediators and sets fundamental limits on orientation-dependent water mediated electron transfer rates.

Keywords

Water-mediated electron transfer; Molecular electronics; Electric field induced switch

Introduction

Charge transport through water is critical to many biological and chemical phenomena, and material processing, including electrocatalysis, biological energy transduction and energy storage. Early studies found that electron tunneling through water between redox active molecules had an exponential decay constant of 1.6–1.7 Å^{-1}, indicating that water supported short-range charge transport[1]. However, X-ray crystallography revealed that water molecules form hydrogen bonds within and between proteins[2–4], which can mediate long-range charge transport in biomolecules, including proteins[4–7] and DNA[8,9], and the fluctuating hydrogen bonds can gate long-range charge transport[10]. Moreover, studies have found that water molecules form low dimensional structures in confined spaces[11,12] and on solid surfaces[13–15], and the tunneling current through a water layer is strongly dependent on the

structure of the layer[16–19]. These findings underscore the importance of the specific nature of water molecules, including their structure and orientation, in charge transport processes, and motivate the investigation of charge transport through single water molecules.

Cryo-temperature experiments find conductance values of water close to $1G_0$ ($G_0 = 2e^2/h = 7.748 \times 10^{-5}$ S, conductance quantum), the conductance for a metal atom in the ballistic transport regime[20,21]. Li et al. also reported this high conductance value (~1 G_0) before and after exposing the gold surface to water at ~10 K and they attributed the high conductance to the formation of gold atomic wires with adsorbed water molecules[22,23]. These studies focused on the ballistic regime and were performed at cryogenic temperatures, while electron transport studies in nature are typically non-ballistic and take place near room temperature. Electron tunneling through liquid water has been measured at room temperature, and trapping and un-trapping of charges have been observed[24], but studies have not measure the conductance of single water molecules bridged between two electrodes.

At room temperature, water molecules tend to form hydrogen bonded clusters[25–27], making it difficult to form a single water molecular junction in the condensed phase. We overcame this challenge by controlling the coverage of water molecules on the electrodes and by measuring the charge transport through single water molecules using the scanning tunneling microscopy (STM) break junction method[28] with a gold substrate and a gold tip. We found that water molecules are less likely to form hydrogen bonded clusters at low surface coverages, which allows an isolated water molecule to bridge between the tip and the substrate electrodes to form a molecular junction. At high surface coverages (e.g., bulk water), hydrogen bonding between water molecules competes with the binding of a water molecule to the electrodes[14,29] and makes it harder to form a molecular junction. We characterized the structure of water molecules on gold electrodes using polarization modulation reflection absorption infrared spectroscopy (PM-RAIRS) and modeled the water-electrode interactions using density functional theory (DFT). Finally, since water molecules have a large electric dipole moment, we examined the influence of molecular orientation on the conductance of a single water molecule by switching its orientation using an electric field.

Results

Water adsorption on gold surfaces and conductance of gold-water-gold junctions

The conductance of molecular junctions was measured using the STM break junction method[28]. A gold STM tip was repeatedly brought into and out of contact with the gold substrate, and the current between the tip and substrate was measured continuously. Individual current vs. tip-substrate distance (I-d) traces were recorded during STM tip retraction. If no molecules bridge between the STM tip and substrate, the current traces show a smooth exponential decay, the characteristic of electron tunneling (black trace in Figure 1C). We first performed the measurements in liquid water, and found no stable molecular junctions were formed. Thousands of current traces were collected to construct a conductance histogram, which does not show any peaks (Figure S1A).

Measuring the monolayer of targeted molecule adsorbed from the gas phase is an alternative way to study single molecular junction besides the measurements in solution. To form a single gold-water-gold molecular junction it requires the controlling of water adsorbed on the gold surface at the monolayer level (Figure 1A). We first characterized the water adsorption on a gold surface in a nitrogen atmosphere under controlled humidity levels using polarization modulation reflection absorption infrared spectroscopy[26] (PM-RAIRS). Figure 1B shows the PM-RAIRS band intensity in the 3000–3700 cm^{-1} region (O-H stretching modes of water, see Figure S2 for IR spectra) versus relative humidity. We observed a quasi-stable region at a relative humidity of ~15–45%, likely due to a monolayer coverage on the surface. This observation is in accordance with our previous results on silicon oxide surfaces[26], and is consistent with other surface characterizations of water on the gold surface under different humidity[27,30,31]. We thus performed STM break junction measurements on the gold surface with 38% relative humidity. Unlike the measurements in liquid water, a plateau in the current-distance trace was frequently observed, indicating the formation of a gold-water-gold molecular junction (blue and red traces in Figure 1C). Thousands of current traces were collected and all of the traces were used to construct a conductance histogram, showing peaks associated with the plateaus (Figure 1D). The peak positions indicate the most probable conductance values for water molecules (see Experimental Procedures for details).

The conductance histogram in Figure 1D reveals two sets of conductance peaks separated by more than an order of magnitude. The low conductance set has a primary peak centered at $2.9 \pm 0.4 \times 10^{-4}$ G$_0$, referred to as the low conductance (LC) state of the water molecule. This primary peak is accompanied by a secondary peak with conductance at ~2× the primary peak conductance (marked LC×2). Such secondary peaks are usually attributed to two molecules in the LC state bridging between the electrodes in parallel (Figure S3 and ref. 28). The high conductance set has a primary peak centered at $2.0 \pm 0.1 \times 10^{-2}$ G$_0$, which is assigned to a high conductance (HC) state of the water molecule. There is also a secondary peak for the HC state with conductance values at ~2× the corresponding primary peak value (denoted HC×2).

The conductance values for the LC and HC-states are both much lower than the values measured at cryogenic temperatures with a platinum electrode[20,21] and Li et al.'s results with gold electrode[22]. Conductance histograms in the regime above 0.1 G$_0$ (Figure S1) do not show pronounced peaks near the previously reported values[20,21]. This is because that temperature, together with the type of metal surface and humidity level (amount of water on the electrode surface) have a large impact on the water-water interactions, and binding and orientation of water molecules on the metal surface (water-electrode contact), which affect 1) the configuration (or geometry) of the molecular junction, 2) electronic coupling between the water molecules and the electrodes, and 3) alignment of the electrodes' Fermi levels with the molecular energy levels. Control experiments in high vacuum (10^{-5} torr) or in pure nitrogen did not find conductance peaks within either the HC or LC ranges (See Figure S4. Also, Figure S1 only shows the 1G$_0$ peak from gold atomic wire, which is consistent with Li et al.'s results[22]), indicating that both the HC and LC peaks arise from water molecules,

Analyzing the length of the conductance plateau (referred to as the stretching length) provides useful information on the binding geometries of water molecules at the electrodes. From the stretching length histograms, the stretching lengths were determined to be 0.09 ± 0.01 nm for the HC state and 0.14 ± 0.01 nm for the LC state (Figure 1E). Both values are shorter than the stretching length of gold atomic junctions formed with water-adsorbed electrodes (~0.64 nm) as reported by Li et al.[22,23], indicating weaker binding between water molecules and the electrodes than between gold atoms in gold atomic junctions.

Humidity dependence of gold-water-gold molecular junctions

To confirm that the HC and LC states arise from a single water molecule, we performed the STM break junction measurements at extremely low relative humidity of ~3%, much lower than the humidity required to form a monolayer coverage[27,30,31]. We observed more pronounced LC peaks at this low humidity, suggesting a single water molecule is being measured. Moreover, forming and breaking water-water hydrogen bonds occur on the picosecond time scale[32,33], so it is unlikely for a water cluster junction to be stable for milliseconds and produce the plateau features in the current-distance traces (Figure 1C). As we show below, the HC state can be switched to a LC state in a single current-voltage sweep. Taken together, these observations suggest that a single gold-water-gold molecular junction is measured in the LC and HC states. The observation of the secondary peaks with conductance values at ~2× the corresponding primary peak values for both the LC and HC-states further evidences that the primary peak arises from single water molecules.

We also measured the dependence of the two conductance states on the relative humidity values (Figure 2A). As the humidity increases, the peak positions of the LC and HC states do not change substantially (see also Figure S5). However, the peak areas, which reflect the populations of the HC and LC states, change significantly. The LC peak area decreases more substantially than the HC peak area, so the ratio of the HC to the LC peak areas increases with humidity (Figure 2B; notice that this ratio does not report the absolute ratio of the population of the two states on the gold surface). The humidity dependence data may be divided into three regimes. In regime I (below ~15% RH), a larger fraction of water is in the LC state, and the fraction in this state decreases rapidly with humidity. In regime II (from ~15% to ~45% RH), the fractions of LC and HC states change little. In regime III (above ~45% RH), the fraction of the LC state decreases rapidly. Both HC and LC states disappeared at high relative humidity of ~67% and 78% (Figure S1). The systematic humidity dependence of the conductance histograms and the consistency of this dependence upon the IR absorption intensity (Figure 1B) further indicate that the LC and HC states arise from water molecules.

To gain insight into the structural and physical origins of the LC and HC states, we performed DFT analysis of water molecules on a 2-layer 3×3 Au (111) surface with periodic boundary conditions (see Experimental Procedures). To simulate Regime I, we initially placed a single water molecule in five different orientations, including parallel (water plane parallel to the gold surface), perpendicular-L and perpendicular-R (where the two hydrogen atoms point toward and away from the gold surface, respectively), and sideway-L and sideway-R (where one O-H bond points away from and one toward the gold surface)

orientations (Figure 2C). The water molecule was then allowed to relax its binding geometry (see Experimental Procedures for details). The sideway-R orientation was unstable in the DFT model and relaxed to the perpendicular-L orientation. The calculation indicates that the parallel orientation is the most stable one (Figure 2D), which is consistent with other calculations[34,35]. In this regime, a single water molecule can be contacted by the STM tip, and retraction of the STM tip brings the water molecule to a perpendicular orientation. As we show below, an electric field can also switch the water molecule from the parallel to the perpendicular orientation. We simulated Regime II by including a water structure formed by water hexamer, a representative type of water cluster on the metal surface[15]. Our DFT calculations revealed two stable conformations: hexamer-L (consisting of parallel and sideway-L orientation structures) and hexamer-R (consisting of parallel and sideway-R orientation structures, Figure 2E). Each of these two water structures contains two layers of water, which are similar to the water bilayer structures[14]. The parallel water layer (as the first layer) has stronger interactions with the gold surface, but the sideway water layer (as the second layer) binds to the parallel water layer through hydrogen bonds and does not have strong interactions with the gold surface. The sideway water layer is slightly further away from the gold surface comparing to parallel water layer (Figure 2E). Since the sideway orientation is unstable in a molecular junction (Figure 2C), we therefore conclude that only water molecules in the parallel orientation can be measured.

We calculated the electronic coupling between the water and the gold electrodes using a finite size gold cluster with adsorbed water molecule (see Experimental Procedures). It was found that the parallel orientation has a stronger coupling than the perpendicular orientation (Figure 2C). The parallel orientation has also a shorter distance between electrodes (shorter tunneling distance) than the perpendicular orientation, which is consistent with the finding that the HC state has a shorter stretching distance that the LC state (Figure 1E). Both the stronger electronic coupling and the shorter tunneling distance indicate that the HC-state of water is in the parallel orientation and the LC-state is in the perpendicular orientation. This is further verified by computing the conductance ratio of the parallel versus the perpendicular orientations. The computed ratio ranges from 3 to 19, depending on the Fermi level energy position (Table S2), which is consistent with the experimental results. The experimental observation of a shorter stretching length for the HC-state than for the LC-state provides further validation of the orientation origin of the HC- and LC-states. The cluster model tends to overestimate the amplitude of the wave function (scaled by $1/\sqrt{N}$ where N is the number of atoms in the cluster), N and thus the coupling strengths, because of the finite size effects of the cluster model. The use of different models for stabilization energy and coupling strength calculations makes it difficult to compare the absolute values obtained by the models, but the relative magnitude comparison consistently indicates that the parallel orientation is more stable than the perpendicular orientation.

Based on the conductance data, IR spectra, and DFT analysis presented above, we provide an explanation for the humidity-dependent behavior of gold-water-gold molecular junctions. In regime I, only a few water molecules are adsorbed on the surface, with most of them in the parallel orientation. This makes it easy for an STM tip to contact a single water molecule from the substrate surface, forming a gold-water molecule-gold junction where the water

molecule can be in parallel or perpendicular orientations (Figure 2C), leading to the HC and LC states, respectively (Figure 2A–B). This explanation is further supported by the extremely low IR intensity of water species, as the parallel water cannot be detected in PM-RAIRS due to image charge screening[36]. STM images also show that the water molecules are largely isolated on the surface[13,37], with low coverage, consistent with the picture above. In regime II, water molecules form a monolayer, where parallel and sideway orientations coexist[14,37] (Figure 2C and 2E). This behavior is further confirmed by IR absorption spectra, as the IR intensity does not change significantly with humidity. The existence of water monolayer has also been confirmed in STM/AFM and spectroscopic studies[13,14,25,38]. Comparing to the low coverage of Regime I, the hydrogen bonds between water molecules in regime II reduces the likelihood for the STM tip to contact a single water molecule and to stretch it into the perpendicular orientation, leading to the larger HC/LC ratio (Figure 2B). In regime III, multiple layers of water molecules begin to form on the surface[13,14], with most water molecules lying flat and bound to their neighbors via hydrogen bonds[25], producing the abrupt increase in the IR intensity. This makes it more difficult to contact a single water molecule with the tip. Conductance histograms at a relative humidity of 67% or 78%, and liquid water too, do not produce peaks with in the same range of the conductance histograms (Figure S1). This further confirms that the HC- and LC- states are caused by tunneling through a single water molecule, instead of tunneling through a water layer or cluster.

Electric field control of water molecule orientation and switching of conductance state

Water is known to have a large electric dipole moment and to respond to electric fields[25,34,39,40], but experimental determination of water dipole moments has been limited to ensemble measurements in the vapor phase[41]. To measure single water molecule dipole moments in the condensed phase, and to examine the switching of water orientations by an electric field, we used an electric field and swept the bias voltage between the STM tip and substrate while monitoring the conductance changes. We first detected a HC-state plateau in the conductance-distance trace (arrows in Figure 3A) during tip retraction at a small bias voltage (−20 mV), which corresponds to the parallel orientation of a water molecule in the junction. We then swept the bias voltage from −20 mV to 2 V, and then back to −20 mV (see Experimental Procedures and ref. 42 for details). For ~70% of the measurements, the conductance drops abruptly to the noise level during the bias voltage sweep, due to breakdown of the molecular junction. For the remaining ~30% of the measurements, the conductance switches from the HC-state to the LC-state at ~1.2 V (arrows in Figure 3B). This is supported by statistical analysis (2D conductance-voltage histogram) that reveals two distinct conduction bands: a HC-band at low bias voltages (0 to ~1.2 V) and a LC-band at high bias voltages (~1.2 V to 2 V). We also reversed the polarity of the bias voltage and observed similar results (Figure S6). Figure 3F sketches an idealized atomic sharp gold tip and atomic flat gold substrate. Experiments have shown that gold atoms are pulled out of the initially flat gold substrate (observed as islands or protrusions on the substrate) in STM break junction measurements, so the tip and substrate electrodes are more symmetric than Figure 3F indicates[43]. Other experiments have shown that the gold tip and substrate alone do not introduce asymmetry in IV characteristics[42]. The LC-state conductance at high bias voltages (Figure 3C) is slightly larger than that at low bias voltages (Figure 2A). This is because of nonlinear I-V characteristics of the LC state (Figure S6). We also performed the

experiment by starting with the LC-state, and found that sweeping the bias voltage did not lead to switching of the conductance to a different level (Figure S6). Previously reported fluctuations in tunneling currents through liquid water are associated with trapping and detrapping of charges in water[24], which are distinct from conductance switching associated with the orientation of single water molecules and the breakdown of the water-electrode contact in the present study.

To understand the electric field-induced water molecule orientation switching, we calculated the energies of a water molecule in both the parallel and perpendicular orientations on the electrodes vs. electric field (Figure 3D). In the absence of the electric field, the parallel orientation is more stable than the perpendicular orientation. (The total energy of the parallel conformation is 2× the free energy of the parallel orientation at the lowest point in Figure 2D. The total energy of the perpendicular conformation is the sum of the free energies from the lowest point of the perpendicular-L and perpendicular-R orientations in Figure 2D). On applying an electric field, the energies of both orientations decrease, but the decrease is more rapid for the perpendicular orientation. The result arises from the interaction of the water dipole ($\boldsymbol{\mu}$) with the electric field ($\mathbf{E}$), with the energy given by $-E \cdot \mu \cdot \cos\theta$, where θ is the angle between the permanent dipole moment and the electric field. The electric field $\mathbf{E}$ includes a component induced by the image dipole in addition to the applied field, and the water dipole includes a contribution from water polarization in addition to its permanent dipole (see Supplemental Experimental Procedures and Figure S7 for details on the calculation). The energies of the parallel and perpendicular orientations cross at ~3.4 V/nm, indicating switching of the water molecule from parallel to perpendicular orientations by the electric field (Figure 3F). The observed switching field is consistent with other theoretical predictions[34,44]. This result also further supports the interpretation that the HC and LC states arise from parallel and perpendicular orientations of water molecules. The percentage of the HC state versus bias voltage (Figure 3C) can also be fitted with an equilibrium population distribution (Supplemental Experimental Procedures). From the fitting (Figure 3E), we obtained the energy difference between parallel and perpendicular orientations in the absence of electric field $U_0 = 0.13 \pm 0.01$ eV (consistent with the results in Figure 2D) and $\mu/d_{gap} = 5.3 \pm 0.1$ D/nm, where μ is the water dipole and d_{gap} is the distance between the two electrodes. Calculations in the literature[25,34,35] and from the present study show that the distance between the oxygen atom and the gold atom for parallel orientations is 0.26–0.30 nm. This yields a dipole moment of 2.7~3.2 D, which is larger than that of an isolated water molecule (1.85 D). This is mainly because the water molecule in the junction is coupled with the two electrodes, and the large electric field can polarize the water molecule. Such large dipole moments were also reported for water in liquid or condensed phase, where individual water molecule is polarized by the surrounding water molecules[45–47]. These theoretical predictions further indicate that the dipole-field interaction can lead to orientation switching of water molecule by an electric field (Figure 3F).

Implications for water-mediated electron transfer reactions

Water molecules can form bridges between proteins to facilitate electron transfer. The conductance in a single molecular junction may be related to the electron transfer rate in the corresponding donor-bridge-acceptor (DBA) system[48]. In a symmetric case where donor and

acceptor are the same, for a typical reorganization energy $\lambda = 0.5$ eV and coupling strengths $\Gamma_D = \Gamma_A = 0.5$ eV with donor and acceptor, we thus predicted the upper and lower limits of electron transfer rates for water bridges with two different orientations ($\beta = 6.2$ nm^{-1} and 13 nm^{-1}, Figure 4A–B and Supplemental Experimental Procedures). These results are consistent with the theoretical and experimental water-mediated electron transfer rates[6,7,49–53]. Moreover, by constructing the 2D conductance-displacement histogram (Figure 4C and Experimental Procedures), we found that the conductance of LC state (perpendicular) is more sensitive to the stretching distance than the HC state (parallel), with decay constants of 5.8 ± 0.2 nm^{-1} and 2.7 ± 0.1 nm^{-1}, respectively. This observation indicates that the electronic coupling between the water molecule and the donor/acceptor depends on the orientation of the water molecules, which is unexpected from the continuous medium picture. The results also reveal how water-mediated electron transfer rates depend on the distance between donor and bridge (d_{D1}), and the distance between acceptor and bridge (d_{NA}, Figure 4A) (which, in turn, depend on the water molecule's orientation). A quantitative comparison between the slope of the stabilization energies in Figure 2D versus distance and the measured decay constant in Figure 4C is difficult to make because of limitations of the potential energy scans and the intrinsic uncertainties in the quantum chemical modeling (including limitations of the basis sets, the DFT functionals, and the size of the supercell that simulates the gold surface). The energy profile in Figure 2D is derived from a potential energy scan with a rigid water orientation (after the orientation optimization), while in the conductance measurements, the water molecule bridges between the two electrodes and stretching can cause orientation variations or orbital energy re-alignments. Effects of this kind may be more pronounced for weakly interacting water molecules (i.e., the perpendicular orientation) because of the smaller stabilization energy and the slower energy dissipation, which produce a steeper slope in the conductance-distance dependence, as shown in Figure 4C.

Discussion

Previous tunneling current measurements[16–18] in liquid water treated water as a continuous tunneling medium, which neglects the discrete nature of single water molecules. In contrast, the present break junction experiments measure conductance by repeatedly creating and breaking single water molecule junctions formed between two electrodes. These studies reveal stepwise changes in the conductance vs. distance traces, associated with distinct peaks in the conductance histograms. This is because that the present work measures a small and controlled amount of water molecules on the electrode, rather than tunneling through bulk water. The studies also found two stable orientations of water molecules and that the corresponding conductance is sensitive to orientation.

Multiple peaks in conductance histograms associated with different binding geometries (e.g. atop and bridge geometries) were usually reported for thiol-gold contacts[54], where a covalent bond is formed between S and Au atoms. In the present case, the water-electrode binding is weak, and we observed a 65-fold difference in the HC and LC states of water molecule, much greater than the conductance differences of the multiple peaks in alkane dithiols. More importantly, we observed switching of HC- to LC- states by an applied electric field, indicating orientation changes. Taken together with the theoretical calculations

and humidity-dependent IR absorption data, our results indicate that HC- and LC-states arise from different water orientations.

Conclusions

In summary, we measured the conductance of single water molecules at room temperature, and observed two distinct values with different orientations: a high conductance ($2.0 \pm 0.1 \times 10^{-2}$ G$_0$) value associated with the parallel orientation and a low conductance ($2.9 \pm 0.4 \times 10^{-4}$ G$_0$) value associated with the perpendicular orientation. Applying an electric field to the water molecule switches it between the parallel and the perpendicular orientations, and leads to conductance switching. These findings are supported by PM-RAIRS analysis and by electronic structure analysis. The studies determine the electrical conductance and the dipole moment - two elementary properties of single water molecules, thus providing a molecular-scale foundation to the understanding of water-mediated electron transfer.

Experimental Procedures

Resources Availability

Lead Contact

Limin Xiang, Limin.Xiang@asu.edu

Materials Availability

No new materials are generated in this study

Data and Code Availability

The data that supports the plots within this paper and other finding of this study are available from the corresponding authors upon reasonable request.

Procedures for measuring conductance:

We performed the STM break-junction experiments in a nitrogen glove box with the relative humidity controlled by delivering water vapor (Mill-Q water, 18.4 MΩ·cm) or by purging the glove box with pure nitrogen (99.998%). The relative humidity was monitored using an Amprobe TH-3 relative humidity temperature meter. A gold tip and a gold substrate were used as the two electrodes. Gold substrates were prepared by thermally evaporating ~160 nm of gold (99.999% purity, Alfa Aesar) onto freshly cleaved mica slides and annealed in ultra-high vacuum (5×10^{-8} torr) for 3 hours. Before each experiment, the gold substrate was flame annealed for 1 min with a hydrogen flame, then mounted onto the STM cell and kept in a vacuum desiccator while being transferred into the nitrogen glove box. The STM tip was freshly cut from gold wire (99.95% purity, Alfa Aesar). For experiments in liquid water and ~78% relative humidity, the STM tip was coated with Apiezon wax to reduce ionic leakage current. A small bias voltage was applied between the tip and substrate (typically 20 mV, otherwise stated). A large number of current–distance traces (~4,000) were recorded in each set of conductance experiment, from which a conductance histogram was constructed with all the traces. Stretching length histogram was constructed by compiling the all distance values for the traces recorded when the conductance was within the full width half-

maximum (FWHM) of the conductance peak including the plateau regime. Two-dimensional conductance-displacement histogram was constructed by aligning all the traces at the conductance value of 0.006 G_0 and projecting them onto a two-dimensional graph.

For measurements in vacuum and in pure nitrogen atmosphere, a gold substrate was flame annealed with butane/hydrogen flame for 30 sec before loading into a vacuum chamber (Janis Research Co.). The chamber was quickly pumped down to ~1×10^{-5} Torr with a turbo pump (Edwards). Current-distance traces were collected with a clean gold substrate at high vacuum first. After that, pure nitrogen gas was introduced into the system and current-distance traces were collected.

Procedures for measuring current-voltage (I-V) relations:

We modified our STM-break junction algorithm to build a histogram of the current transient in real time in order to detect plateaus before the corresponding molecular junction broke[42]. If a plateau was detected, the piezo modulation was paused and the bias was swept over a certain range up to ±2 V. Once the bias sweep was completed, the piezo continued to ramp away the STM tip from the substrate and the break junction cycle was repeated. In this method, approximately 3000 current-voltage (IV) traces were recorded, from which the 2D conductance-voltage (G-V) histogram was constructed[42].

Polarization-modulation reflection absorption infrared spectroscopy:

PM-RAIRS spectra were collected to investigate the water adsorption on gold surfaces. The spectra were collected using a ThermoNicolet Nexus 670 spectrometer with a MCT-A detector. Based on the metal selection rules of IR reflection, PM-RAIRS is able to detect the adsorbed species without the interference of the gas phase. The sum and difference of the p- and s- polarized reflection IR were collected simultaneously. The difference (p-s) signal carries only the information from the adsorbates with the perpendicular portions of its dipole change to the surface (due to the metal surface selection rule[36]), while the sum (p+s) signal contains both the adsorbates and gas phase molecules. By normalizing these two signals, the spectrum of the adsorbed water can be obtained. Vapor phase environment with a controlled relative humidity was achieved in a continuous flow chamber by mixing the dry N_2 and saturated water vapor with a desired proportion. The saturated water stream was produced by flowing the carrier gas (N_2) through a column filled with water (>18 MΩ·cm).

Computational methods:

The structure of a single water molecule was optimized on a 2-layer gold (111) surface with periodic boundary conditions (Figure 2C–D). The periodic supercell contained a 3×3 gold surface and a single water molecule was initially placed in the parallel (water plane parallel to the gold surface), perpendicular-L (two O-H bonds pointing towards gold surface), perpendicular-R (two O-H bonds pointing away from gold surface), sideway-L (one O-H bond pointing away from the gold surface) and sideway-R (one O-H bond pointing towards the gold surface) positions (see Figure 2C). To reduce the interaction between the mirror surfaces, a 20 Å vacuum layer was added to the supercell in the direction perpendicular to the surface. PBE-GGA pseudo-potential with the DZP basis set was used to describe the atomic interaction and the simulation was conducted using the SIESTA package. The choice

of the PBE functional was based on its superb performance in the description of the electronic properties of the Au cluster and water absorption on the gold surface[34,35]. In particular, a recently computational study[34] showed that the adsorption energetics and the electrostatic interactions and between water and gold with/without the electric field were well described by the PBE functional. Gold atoms were constrained while relaxing the water molecules. After we found the optimized position of the water molecules, we manually pulled the water molecules away from the surface with a step size of 0.1 Å. At each step, the total energy was calculated. The structure of the water monolayer was simulated using the same method. The initial positions of the water molecules were alternatively placed in the parallel and sideway orientations. Figure 2E shows the repeating unit of the water monolayer (a honeycomb-like structure) after the relaxations. This calculation shows that the alternating parallel/sideway structure is energetically more stable because of the hydrogen bonding interactions.

We computed the coupling strengths (shown as the numbers in Figure 2C) based on a finite size cluster model without periodic boundary conditions. The clusters were chosen to be sufficiently large with hydrogen atoms added at the boundary to minimize the impact of cutting the slabs. The effective molecule–electrode coupling was described by the spectral density

$$\Gamma(\varepsilon) \;=\; 2\pi \, \Sigma_n |V_n|^2 \, \delta(\varepsilon - \varepsilon_n), \qquad \text{Eq. 1}$$

In the present case (water on gold), we approximate $\varepsilon = E_{HOMO}$ as the HOMO energy of water.

We also approximated the Dirac d function as,

$$\delta(x) \;=\; \lim_{\sigma \to 0} \frac{1}{\sqrt{2\pi\sigma^2}} \exp\!\left(-\frac{x^2}{2\sigma^2}\right), \qquad \text{Eq. 2}$$

We compared the effective coupling between the water and the electrode at different σ values for different water orientations. PBE was used to optimize the structure and construct the supercell by extending in each lattice vector direction with one periodicity. Gold atoms were capped with Hydrogen atoms at the edges and on the bottom surface. We computed the effective coupling using the same PBE-GGA DFT functionals as above with relativistic effective potentials[55] for gold, 6–31G(d) for H_2O and STO-3G for the capping H atoms. Standard DFT based block-diagonalization methods are used to approximate the diabatic couplings using the adiabatic electronic Hamiltonian constructed from ab initio or DFT quantum chemical computations. V_n is the off-diagonal matrix element from the block-diagonalized Kohn-Sham matrix. The computed results are summarized in Table S1. The coupling strength values shown in Figure 2C were calculated with a σ value of 0.025 eV. Computational methods for calculating the conductance ratios are provided in Supplemental Experimental Procedures.

Supplementary Material

Refer to Web version on PubMed Central for supplementary material.

Acknowledgments

References

1. Ponce A, Gray HB & Winkler JR (2000). Electron Tunneling through Water: Oxidative Quenching of Electronically Excited Ru(tpy)22+ (tpy = 2,2':6,2' '-terpyridine) by Ferric Ions in Aqueous Glasses at 77 K. J. Am. Chem. Soc 122, 8187–8191.

2. Sun T, Lin F-H, Campbell RL, Allingham JS & Davies PL (2014). An Antifreeze Protein Folds with an Interior Network of More Than 400 Semi-Clathrate Waters. Science 343, 795. [PubMed: 24531972]

3. Lee J & Kim S-H (2009). Water polygons in high-resolution protein crystal structures. Protein Sci. 18, 1370–1376. [PubMed: 19551896]

4. Antonyuk SV, Han C, Eady RR & Hasnain SS (2013). Structures of protein–protein complexes involved in electron transfer. Nature 496, 123. [PubMed: 23535590]

5. Lin J, Balabin IA & Beratan DN (2005). The Nature of Aqueous Tunneling Pathways Between Electron-Transfer Proteins. Science 310, 1311–1313. [PubMed: 16311331]

6. Chakrabarti S, Parker MFL, Morgan CW, Schafmeister CE & Waldeck DH (2009). Experimental Evidence for Water Mediated Electron Transfer Through Bis-Amino Acid Donor–Bridge–Acceptor Oligomers. J. Am. Chem. Soc 131, 2044–2045. [PubMed: 19173584]

7. Tezcan FA, Crane BR, Winkler JR & Gray HB (2001). Electron tunneling in protein crystals. Proc. Natl. Acad. Sci. U. S. A 98, 5002–5006. [PubMed: 11296248]

8. Khesbak H, Savchuk O, Tsushima S & Fahmy K (2011). The Role of Water H-Bond Imbalances in B-DNA Substate Transitions and Peptide Recognition Revealed by Time-Resolved FTIR Spectroscopy. J. Am. Chem. Soc 133, 5834–5842. [PubMed: 21446714]

9. Barnett RN, Cleveland CL, Joy A, Landman U & Schuster GB (2001). Charge Migration in DNA: Ion-Gated Transport. Science 294, 567. [PubMed: 11641491]

10. Kretchmer JS et al. (2018). Fluctuating hydrogen-bond networks govern anomalous electron transfer kinetics in a blue copper protein. Proc. Natl. Acad. Sci. U. S. A 115, 6129. [PubMed: 29844178]

11. Algara-Siller G et al. (2015). Square ice in graphene nanocapillaries. Nature 519, 443. [PubMed: 25810206]

12. Xu K, Cao P & Heath JR (2010). Graphene Visualizes the First Water Adlayers on Mica at Ambient Conditions. Science 329, 1188–1191. [PubMed: 20813950]

13. Maier S & Salmeron M (2015). How Does Water Wet a Surface? Acc. Chem. Res 48, 2783–2790. [PubMed: 26418288]

14. Carrasco J, Hodgson A & Michaelides A (2012). A molecular perspective of water at metal interfaces. Nat. Mater 11, 667–674. [PubMed: 22825022]

15. Michaelides A & Morgenstern K (2007). Ice nanoclusters at hydrophobic metal surfaces. Nat. Mater 6, 597–601. [PubMed: 17572679]

16. Vaught A, Jing TW & Lindsay SM (1995). Non-exponential tunneling in water near an electrode. Chem. Phys. Lett 236, 306–310.

17. Galperin M, Nitzan A & Benjamin I (2002). Numerical Simulations of Electron Tunneling Currents in Water. J. Phy. Chem. A 106, 10790–10796.

18. Schmickler W (1995). Tunneling of electrons through thin layers of water. Surf. Sci 335, 416–421.

19. Albrecht T (2012). Electrochemical tunnelling sensors and their potential applications. Nat. Commun 3, 829. [PubMed: 22569373]

20. Tal O, Krieger M, Leerink B & van Ruitenbeek JM (2008). Electron-Vibration Interaction in Single-Molecule Junctions: From Contact to Tunneling Regimes. Phys. Rev. Lett 100, 196804. [PubMed: 18518474]

21. Tal O et al. (2009). Molecular signature of highly conductive metal-molecule-metal junctions. Phys. Rev. B 80, 085427.

22. Li Y, Kaneko S, Fujii S, Nishino T & Kiguchi M (2017). Atomic structure of water/Au, Ag, Cu and Pt atomic junctions. PhysChemChemPhys 19, 4673–4677.

23. Li Y et al. (2015). Electrical conductance and structure of copper atomic junctions in the presence of water molecules. PhysChemChemPhys 17, 32436–32442.

24. Boussaad S et al. (2003). Discrete tunneling current fluctuations in metal–water–metal tunnel junctions. J. Chem. Phys 118, 8891–8897.

25. Velasco-Velez J-J et al. (2014). The structure of interfacial water on gold electrodes studied by x-ray absorption spectroscopy. Science 346, 831–834. [PubMed: 25342657]

26. Asay DB & Kim SH (2005). Evolution of the Adsorbed Water Layer Structure on Silicon Oxide at Room Temperature. J. Phys. Chem. B 109, 16760–16763. [PubMed: 16853134]

27. Demirdjian B, Bedu F, Ranguis A, Ozerov I & Henry CR (2018). Water Adsorption by a Sensitive Calibrated Gold Plasmonic Nanosensor. Langmuir 34, 5381–5385. [PubMed: 29678113]

28. Xu B & Tao NJ (2003). Measurement of Single-Molecule Resistance by Repeated Formation of Molecular Junctions. Science 301, 1221–1223. [PubMed: 12947193]

29. Tatarkhanov M et al. (2009). Metal- and Hydrogen-Bonding Competition during Water Adsorption on Pd(111) and Ru(0001). J. Am. Chem. Soc 131, 18425–18434. [PubMed: 19947628]

30. Lee S & Staehle RW (1996). Study of Water Adsorbed on Gold: Assessment of Polarization Model. Mater. Trans. JIM 37, 1768–1773.

31. Guo LQ, Zhao XM, Bai Y & Qiao LJ (2012). Water adsorption behavior on metal surfaces and its influence on surface potential studied by in situ SPM. Appl. Surf. Sci 258, 9087–9091.

32. Rey R, Møller KB & Hynes JT (2002). Hydrogen Bond Dynamics in Water and Ultrafast Infrared Spectroscopy. J. Phys. Chem. A 106, 11993–11996.

33. Luzar A & Chandler D (1996). Hydrogen-bond kinetics in liquid water. Nature 379, 55–57.

34. Huzayyin A, Chang JH, Lian K & Dawson F (2014). Interaction of Water Molecule with Au(111) and Au(110) Surfaces under the Influence of an External Electric Field. J. Phys. Chem. C 118, 3459–3470.

35. Carrasco J, Klimeš J & Michaelides A (2013). The role of van der Waals forces in water adsorption on metals. J. Chem. Phys 138, 024708. [PubMed: 23320714]

36. Greenler RG (1966). Infrared Study of Adsorbed Molecules on Metal Surfaces by Reflection Techniques. J. Chem. Phys 44, 310–315.

37. Mitsui T, Rose MK, Fomin E, Ogletree DF & Salmeron M (2002). Water Diffusion and Clustering on Pd(111). Science 297, 1850. [PubMed: 12228712]

38. Björneholm O et al. (2016). Water at Interfaces. Chem. Rev 116, 7698–7726. [PubMed: 27232062]

39. Toney MF et al. (1994). Voltage-dependent ordering of water molecules at an electrode-electrolyte interface. Nature 368, 444–446.

40. Osawa M, Tsushima M, Mogami H, Samjeské G & Yamakata A (2008). Structure of Water at the Electrified Platinum–Water Interface: A Study by Surface-Enhanced Infrared Absorption Spectroscopy. J. Phys. Chem. C 112, 4248–4256.

41. Birnbaum G & Chatterjee SK (1952). The Dielectric Constant of Water Vapor in the Microwave Region. J. Appl. Phys 23, 220–223.

42. Guo S, Hihath J, Díez-Pérez I & Tao N (2011). Measurement and Statistical Analysis of Single-Molecule Current–Voltage Characteristics, Transition Voltage Spectroscopy, and Tunneling Barrier Height. J. Am. Chem. Soc 133, 19189–19197. [PubMed: 21991939]

43. He J et al. (2006). Measuring single molecule conductance with break junctions. Faraday Discus. 131, 145–154.

44. Pedroza LS, Brandimarte P, Rocha AR & Fernández-Serra MV (2018). Bias-dependent local structure of water molecules at a metallic interface. Chem. Sci 9, 62–69. [PubMed: 29629074]

45. Silvestrelli PL & Parrinello M (1999). Structural, electronic, and bonding properties of liquid water from first principles. J. Chem. Phys 111, 3572–3580.

46. Badyal YS et al. (2000). Electron distribution in water. J. Chem. Phys 112, 9206–9208.

47. Gregory JK, Clary DC, Liu K, Brown MG & Saykally RJ (1997). The Water Dipole Moment in Water Clusters. Science 275, 814. [PubMed: 9012344]

48. Nitzan A (2001). A Relationship between Electron-Transfer Rates and Molecular Conduction. J. Phy. Chem. A 105, 2677–2679.

49. van Amsterdam IMC et al. (2002). Dramatic modulation of electron transfer in protein complexes by crosslinking. Nat. Struct. Mol. Biol 9, 48–52.

50. Miyashita O, Okamura MY & Onuchic JN (2005). Interprotein electron transfer from cytochrome c2 to photosynthetic reaction center: Tunneling across an aqueous interface. Proc. Natl. Acad. Sci. U. S. A 102, 3558. [PubMed: 15738426]

51. Migliore A, Corni S, Di Felice R & Molinari E (2007). Water-Mediated Electron Transfer between Protein Redox Centers. J. Phys. Chem. B 111, 3774–3781. [PubMed: 17388538]

52. Cárdenas DJ, Cuerva JM, Alías M, Buñuel E & Campaña AG (2011). Water-Based Hydrogen-Atom Wires as Mediators in Long-Range Proton-Coupled Electron Transfer in Enzymes: A New Twist on Water Reactivity. Chem. Eur. J 17, 8318–8323. [PubMed: 21671300]

53. Migliore A, Corni S, Di Felice R & Molinari E (2006). Water Effects on Electron Transfer in Azurin Dimers. J. Phys. Chem. B 110, 23796–23800. [PubMed: 17125342]

54. Chen F, Li X, Hihath J, Huang Z & Tao N (2006). Effect of Anchoring Groups on Single-Molecule Conductance: Comparative Study of Thiol-, Amine-, and Carboxylic-Acid-Terminated Molecules. J. Am. Chem. Soc 128, 15874–15881. [PubMed: 17147400]

55. Ross RB et al. (1990). Ab initio relativistic effective potentials with spin–orbit operators. IV. Cs through Rn. J. Chem. Phys 93, 6654–6670.

(1) A Progress and Potential statement no longer than 1,000 characters, including spaces

Extensive studies have shown that water can mediate electron transfer by forming water bridges. However, the electrical conductance of a single water molecule at room temperature remains unknown. Here, we studied single water molecular junctions via conductance measurements, theoretical analysis and infrared spectroscopy. We found two states associated with single water molecular conductance, corresponding to two orientations in the molecular junctions. These two states set fundamental limits on water mediated electron-transfer rates. We further switched the orientations via an external electric field and determined the single water dipole moment. Our work provides a molecular-scale foundation to understand water-mediated electron transfer in chemistry and material science, and motivates future investigations of energy transduction at the water-electrode interfaces.

(2) 3–4 Highlights of no more than 85 characters each, including spaces

1. Two single-water molecule conductance states were found

2. Theoretical analysis and IR spectroscopy revealed two water orientations

3. An external electric field switched water from high to low conductance states

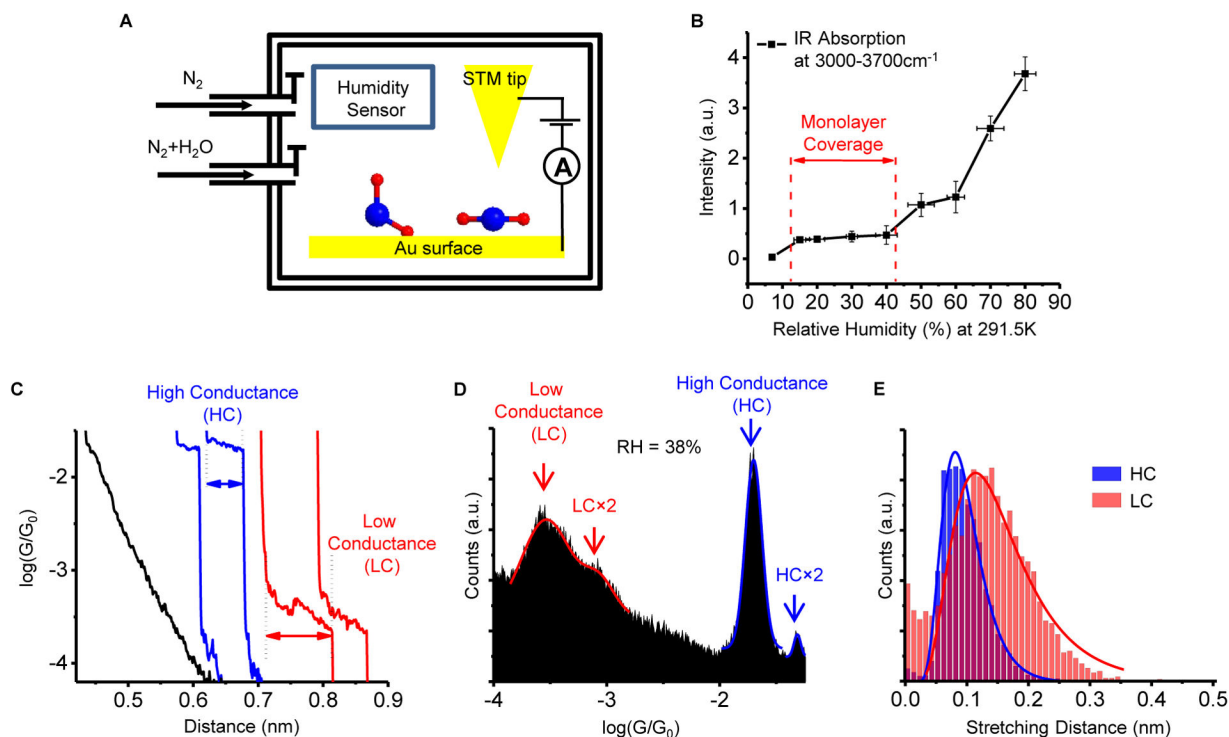4. The two states set fundamental limits on water mediated electron transfer rates

Figure 1. Conductance measurements of water molecular junctions.

(A) Schematic illustration of the experimental setup. A gold STM tip is brought into contact with a water molecule-covered gold substrate and then retracted from the substrate. During this process, a water molecule can bridge between the two electrodes, forming a gold-water-gold molecular junction. **(B)** PM-RAIRS analysis was performed on the gold surface with controlled relative humidity. Plotting the absorption band intensity in the region of 3000–3700 cm^{-1} (O-H stretching modes of water) versus the relatively humidity shows a quasi-stable region from ~15% to ~45%, likely due to a monolayer coverage. The error bars in the IR data are the standard deviations of more than 3 sets of experiments. **(C)** Representative current-distance (I-d) traces during the retraction process of STM tip in panel A show conductance plateaus in a high conductance (HC) state (blue) and a low conductance (LC) state (red). I-d traces without forming a molecular junction between the tip and the substrate show smooth exponential decay (black). **(D)** A representative conductance histogram with a relative humidity of ~38% constructed from ~4000 I-d traces show a HC peak and a LC peak, peaks at 2× the HC and LC values (HC×2 and LC×2) that originate from two water molecules bridging between the electrodes in parallel. The solid lines are Gaussian fits to the histograms, and the peak positions from the fits are taken as the conductance values. **(E)** Stretching length histograms of the HC and LC states, where the solid lines are fits with a lognormal distribution. The stretching length is the distance over which a molecular junction can be extended before breakdown (arrows marked in panel **C**). See also Figure S2, Figure S3 and Figure S4.
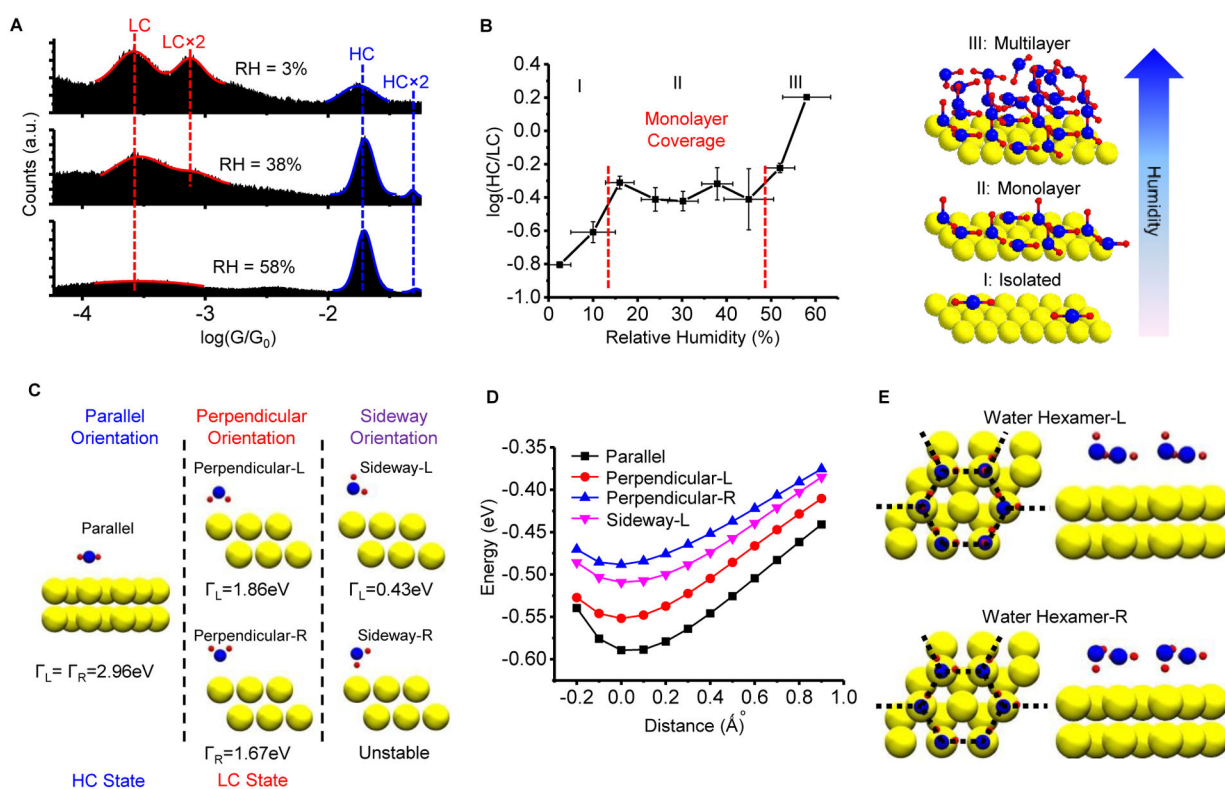
Figure 2. Dependence of water orientations on relative humidity (surface coverage of water).
(**A**) Conductance histograms at 3%, 38% and 58% relative humidity (RH). The peak
positions of the HC and LC states do not change, but their peak areas vary with relative
humidity. (**B**) The ratio of the HC- to the LC- peak areas (black points) versus relative
humidity, where "I", "II" and "III" mark three regimes. I: a few water molecules, II: a
monolayer coverage, III: water multilayers on the gold surface. The error bars in the
conductance data are from the fitting errors. The errors bars in the humidity are from the
reading errors of the humidity sensor. Model illustrations (right of the plots) are presented to
show water molecules on a surface in the corresponding three regimes. (**C**) Optimized
orientations of an isolated water molecule on a gold electrode. Calculations indicate that the
parallel water orientation provides stronger electronic coupling (Γ) between electrodes than
the perpendicular orientation. (**D**) Calculated total energies of the four stable orientations
shown in panel **C** as a function of the Au-O distance indicate that the parallel orientation is
most stable. (**E**) Optimized water structures at monolayer coverage on a gold surface with a
repeating unit of either hexamer-L (consists of parallel and sideway-L orientations) or
hexamer-R (consists of parallel and sideway-R orientations), which is similar to the water
bilayer structures[14]. Left: top view; Right: side view. Only the parallel orientation in the
bilayer structures can form a stable molecular junction and be measured. See also Figure S1,
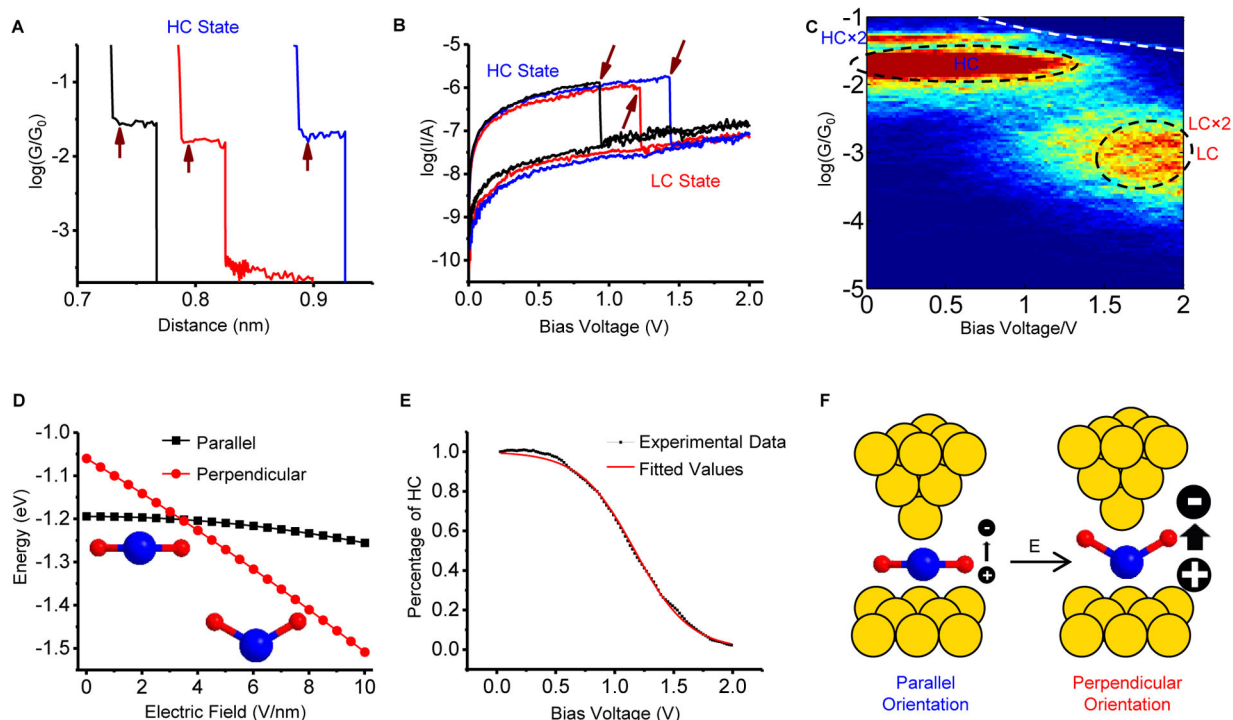Figure S5, Table S1 and Table S2.

Figure 3. Electric field induces a change in water orientation.
(**A**) Conductance vs. distance traces. When a plateau is detected (meaning that a water molecule is bridged between the tip and substrate), the tip is fixed and bias voltage is swept (marked by the arrows). (**B**) Representative current-voltage (I-V) curves show the switching from the HC state to the LC state as marked by arrows at high bias voltage. (**C**) 2D conductance-voltage (G-V) histogram constructed from thousands of I-V curves shows a high conduction band at low bias voltages and a low conduction band at high bias voltages (Circled area). The white dashed line marks the saturation of the current amplifier. (**D**) The dependence of the total energy (adopted from Figure 2D) on the external electric field for the parallel (blue) and the perpendicular (red) orientations, with a crossover at ~3.4 V/nm. (**E**) Fitting the percentage of HC state versus bias voltage in panel **C** with the population distribution under equilibrium gives an estimation of water dipole moment (see text for details). (**F**) Switching of a water molecule from the parallel to the perpendicular orientation at high electric field as predicted in **D** and observed as a drop in the current in **B**. The atomic sharp STM tip and atomic flat substrate shown in the carton are an over simplification for illustration. See also Figure S6 and Figure S7.
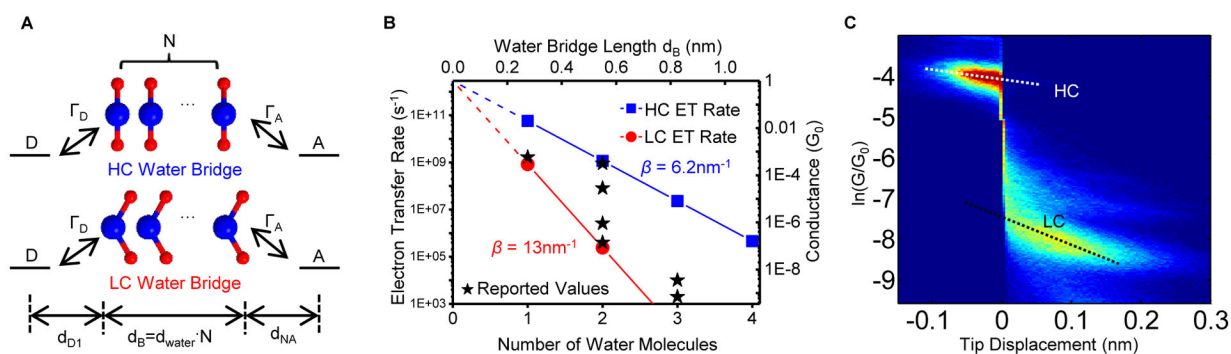
Figure 4. A proposed model for water-mediated electron transfer.
(A) A model donor-bridge-acceptor (DBA) system consists of N water molecules in either HC state or LC state as the bridge. **(B)** Electron transfer rate vs. N for the water molecules in HC state (blue) and LC state (red), respectively, which set two limits on the electron transfer rate. Experimental and theoretical electron transfer rates from literature are plotted here as black stars for comparison. **(C)** Two-dimensional conductance-displacement histogram shows that the LC state conductance is more sensitive to distance than the HC state, indicating different electronic couplings between the donor (acceptor) and water molecules in the parallel and perpendicular orientations. Note that the y-axis is on a natural logarithm scale to better visualize the exponential decay constant. Dash line indicates the slope of the decay.